

Utilization of Selected Area Electron Diffraction Patterns for Characterization of Air Submicron Particulate Matter Collected by a Thermophoretic Precipitator

John J. Bang, Elizabeth A. Trillo, and Lawrence E. Murr

Department of Metallurgical and Materials Engineering and Center for Environmental Resource Management, University of Texas, El Paso, Texas

ABSTRACT

A thermophoretic precipitator (TP) that uses a novelty of direct sampling of ambient air particulate matter (PM) onto transmission electron microscopy (TEM) grids was designed and utilized to determine its potential applicability for the collection and consequent qualitative analyses of representative PM in the air, especially those with aerodynamic diameter less than 1 μm ($\text{PM}_{1.0}$). After a calibration process, preliminary field tests were performed under different weather conditions, locations, and time frames. TEM, selected area electron diffraction (SAED), and electron energy-dispersive X-ray spectrometry (EDS) analyses were performed on individual samples, and chemical species were analyzed. During this investigation, individual air PM with different sizes ranging from 10 μm to 10 nm for TEM analysis was collected. Two observations were made: (1) a large fraction of collected particulates were aggregates of very small particles of both organic and inorganic origin, and (2) a large fraction of the collected particulates were crystalline or polycrystalline. This study has demonstrated, by utilization of SAED patterns from TEM on air particles collected by a TP, the potential to analyze and identify individual air PM in a nanometer regime qualitatively by combining SAED and EDS data.

IMPLICATIONS

Many researchers working in air pollution-related fields have focused on the sizes and intrinsic characteristics of PM and aerosols in ambient air as a way to protect public health. In recent years, however, more and more studies in both the engineering and healthcare fields have supported the necessity of qualitative characterizations of PM. The authors of this article believe that future regulations about air pollution control should embrace some qualitative aspects of air pollutants through studies like this experiment to be more complete and effective.

INTRODUCTION

The harmful effects of anthropogenic air pollutants, especially ambient air particulate matter (PM), on the human respiratory system have been shown in the past. Positive associations between the levels of exposure to PM, in terms of mass, and mortality rates also have been demonstrated.¹ As evidence of the more harmful effects of ultrafine PM accumulates, the focus has been directed from the issue of high-level mass exposure to that of high surface area-to-volume ratio for the measure of potential toxicity. In a recent clinical study, data justifying the effort to identify the sources of $\text{PM}_{2.5}$ (PM with aerodynamic diameter equal to or less than 2.5 μm) and qualitatively characterize the individual particles of interest in the air were presented.² In that study, more than 90% of the particles deposited in every airway site in the lung had aerodynamic diameters less than 2.5 μm .

Extensive research about the inorganic components of the PM_{10} and $\text{PM}_{2.5}$ has revealed information about characteristics of ambient PM. For example, crystalline/metal components, rather than corresponding amorphous structures of air particulates, seemed to be more damaging to the lung epithelial lining cells.^{3,4} Detrimental effects of reactive oxygen species generated by inorganic minerals and metal constituents of airborne PM on airway epithelia also have been observed.⁵⁻⁷ Furthermore, the potential role of transition metal oxides as a catalyst for generation of ambient PM was demonstrated.⁸

Recently, investigation revealed that ultrafine particles (aerodynamic diameter less than 0.1 μm) are more strongly associated with mortality or morbidity rate than are fine ($\text{PM}_{1.0}$) or coarse particles ($\text{PM}_{2.5-10}$). In one study,⁹ ultrafine particles impaired macrophage phagocytosis to a greater extent than did fine particles compared on a mass basis. From these studies, it seems that some constituents of nanoparticles, either by themselves or in agglomerated forms of millimeter size, play major roles in damaging lung tissues.

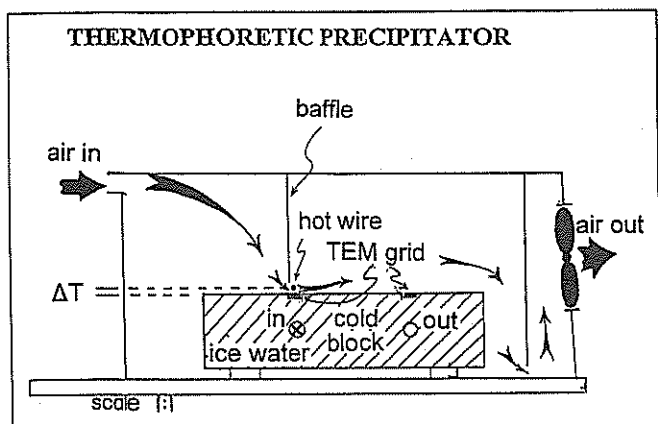


Figure 1. TP side view.

The effort of characterizing ambient aerosol particles for various reasons traces back to the 1930s. Green and Watson¹⁰ at that time built a thermophoretic precipitator (TP) based on theoretical work from Einstein.¹¹ It was used for air dust collection in work places to monitor air quality in work places. An analysis of urban aerosols by

using combined lidar, SEM, and X-ray microanalysis was performed by Frejafon et al.¹² In their study, the composition of different sized aerosols was presented. Ebert et al.¹³ also characterized approximately 3000 aerosol particles in the North Sea area in terms of size, morphology, and chemical composition. Chemical analyses on ice-forming nuclei in the air of New Mexico regions were performed to reveal the mechanisms of ice particle formation.¹⁴ Lately, similar attempts to reveal the elemental composition and morphology of ice-crystal residual particles in cirrus clouds and contrails was made.¹⁵ Analyses of interplanetary dust were also performed.¹⁶ The original TP has been modified throughout the years for better analyses of small particles in the air. One application of TP for characterizing ultrafine PM was also well demonstrated.¹⁷ For bulk chemical and physical analyses, automated computer techniques using filters have also been used.¹⁸ In that study, air samples were collected on filters and categorized in different groups depending on chemical composition for component analyses. However, few

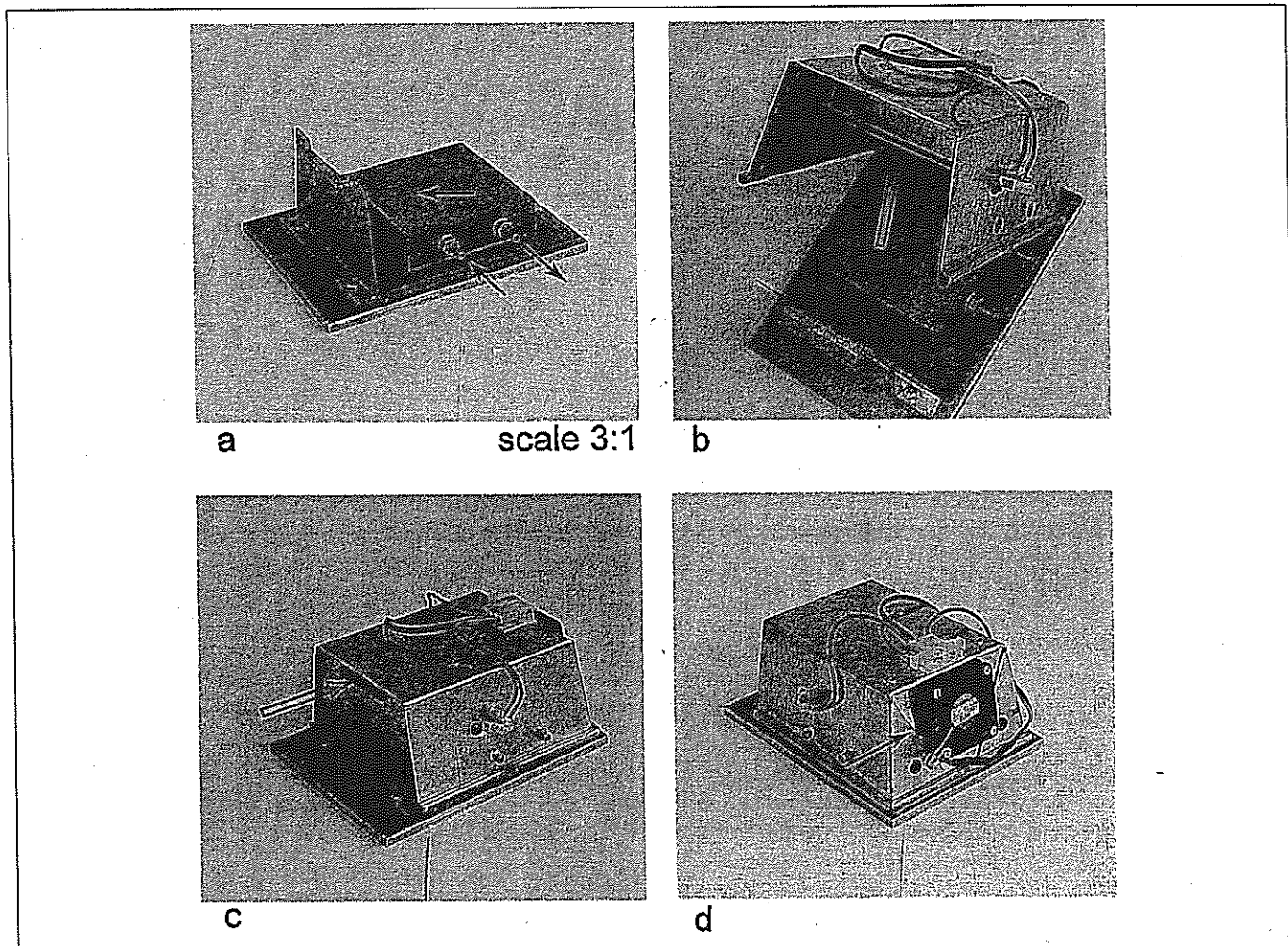


Figure 2. TP: (a) Six grid positions (one is indicated by an arrow) on a copper block with two cooling water coils that are indicated by two arrows. (b) Tungsten hot wire indicated by an arrow. (c) TP with a cover. The air inlet is shown in the front arrow. (d) Rear fan is indicated by an arrow.

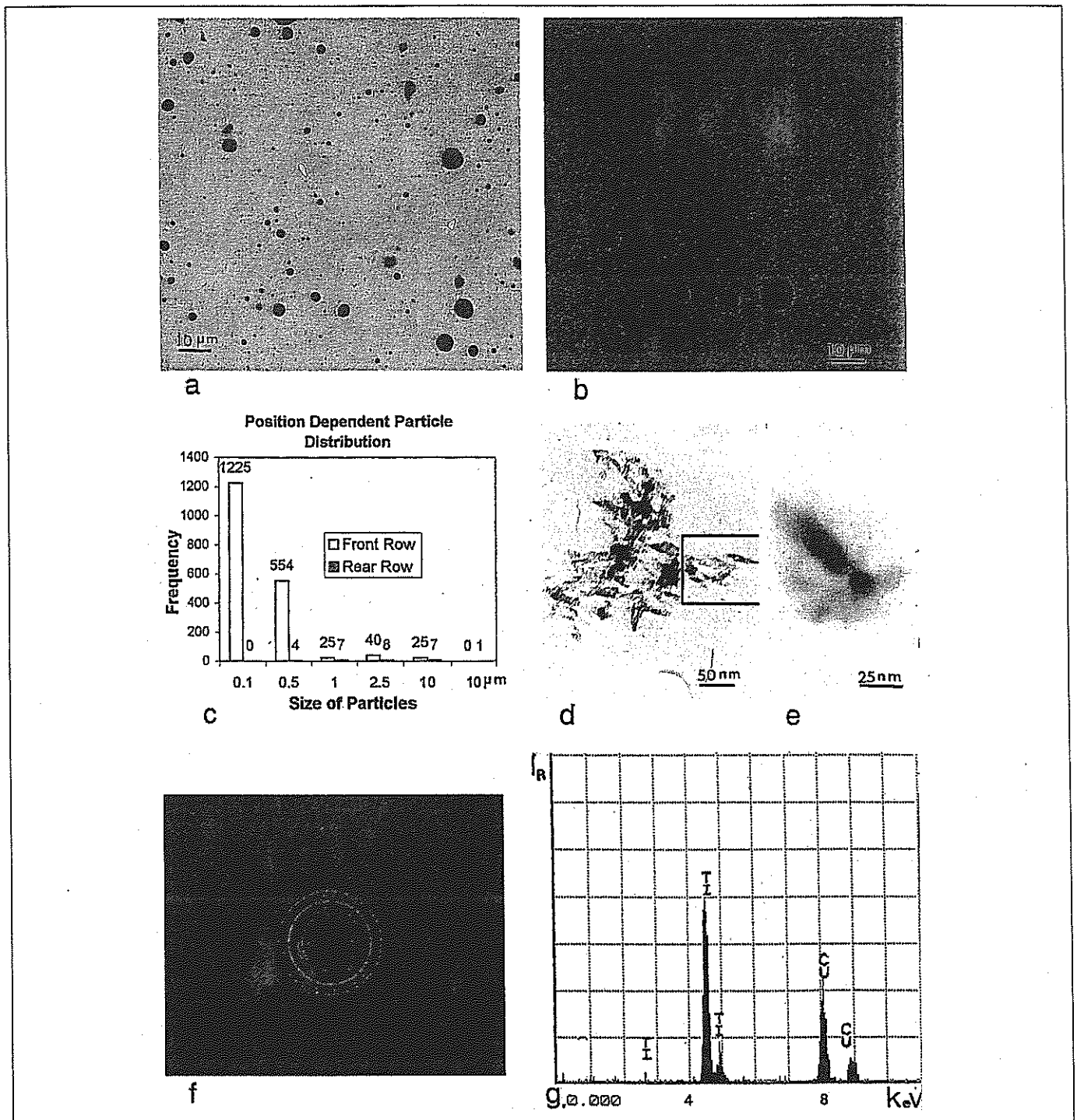


Figure 3. Calibration by smoke particles of burning papers (a, b, and c), TiO_2 rutile powder (d, e, f, and g). (a) Collection from front row. (b) Collection from rear row. (c) Comparison of collection efficiency between two rows. (d) Aggregate of TiO_2 rutile powder. (e) Individual TiO_2 rutile powder (approximate $10 \times 50 \text{ nm}$ dimension). (f) SAED on (d), only the area in the bracket was exposed for SAED. (g) EDS for the same are used for SAED in (d).

studies have focused on identifying the specific structure, size, morphology, crystallinity, and chemical composition of individual ultrafine or nanoparticles, or any particulates, for that matter. As presented in studies conducted by the Health Effects Institute,¹⁹ it became imperative to characterize and, if possible, identify individual particles in the nanoparticle regime.

Transmission electron microscopy (TEM) can provide information to help identify particulates in terms of chemistry and crystallography as well as morphology and size distributions. Airborne PM collected on filters or other common filtration and collection devices is often limited in its ability to be analyzed, mainly because of its complexity and reduced ability to transfer collected

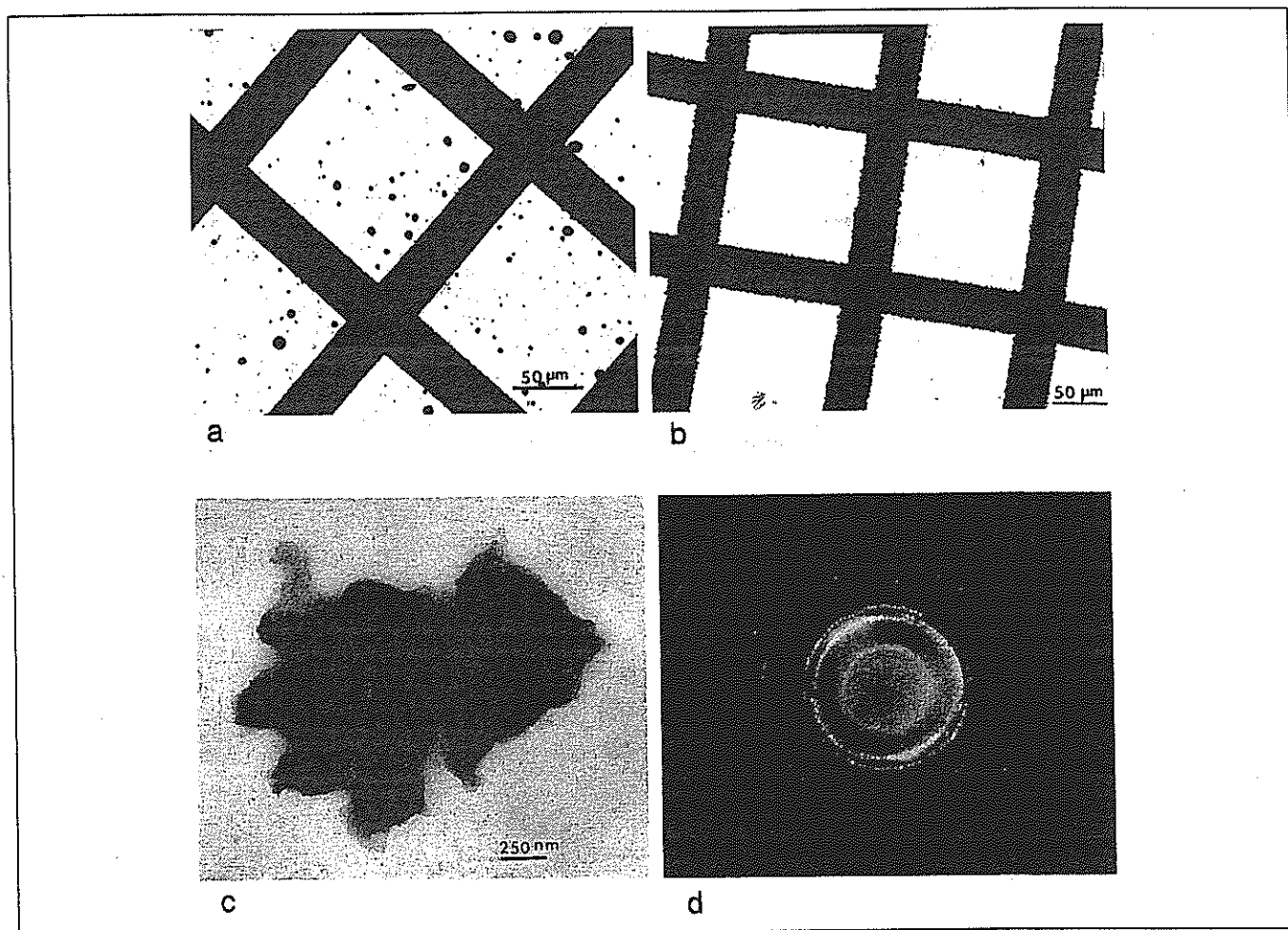


Figure 4. Sample collection on grids: (a) Particles from burning paper on coated copper grid mesh (TEM). (b) Cigarette smoke particulates (TEM). (c) Cigarette smoke particle enlarged (TEM). (d) SAED for cigarette smoke particle in (c) showing polycrystallinity. Ambient air samples collected during a late evening at El Paso.

particulates to a medium that facilitates viewing by TEM, even though quantification of collected PM can be made possible. Crystallography seems to be more informative, because catalytic activity is related to specialized atomic arrangements creating chemically active surface sites or regions.^{20,21} Consequently, it may not be critical to simply verify shapes, sizes, or even determine chemical speciation for the purpose of revealing associated mechanisms or steps for the generation process of toxic nanoparticles or agglomeration process of nanoparticles. Thus, a convenient collection scheme placing unprocessed small individual nanoparticles on an electron-transparent surface or sampling environment specific to TEM analysis poses special advantages, and can afford the opportunity for high-resolution of nanoparticles of our interest.

For this investigation, a portable TP was designed and fabricated to collect ultrafine, representative airborne PM for qualitative TEM analysis using data from selected area electron diffraction (SAED) patterns of examined particles, such that characteristic morphology, structure, crystallography, and chemical composition of individual

ambient PM would be determined for possible identification of the particles examined. After a calibration process using smoke from burning papers and cigarettes and TiO₂ rutile nano-size powder, a series of field tests at different time frames during different weather conditions was performed to illustrate the ability of this collection and analysis methodology in a preliminary way. Smoke aerosol size distribution and some bright field STEM images are shown in Figures 3 and 4.

EXPERIMENTAL METHOD

Theory

Gas molecules in hot regions have higher momentum with high kinetic energy than do those in cold regions. Consequently, greater force will be generated in hot regions than in cold regions after collision of molecules. As a result, particles have a tendency to move from a hot to a cold region. For both small (Knudsen number, $Kn \gg 1$) and large ($Kn \ll 1$) aerosols, the same concept is applied.²² This concept of thermophoresis has been used to build a series of TPs. In 1935, Green and Watson¹⁰ found

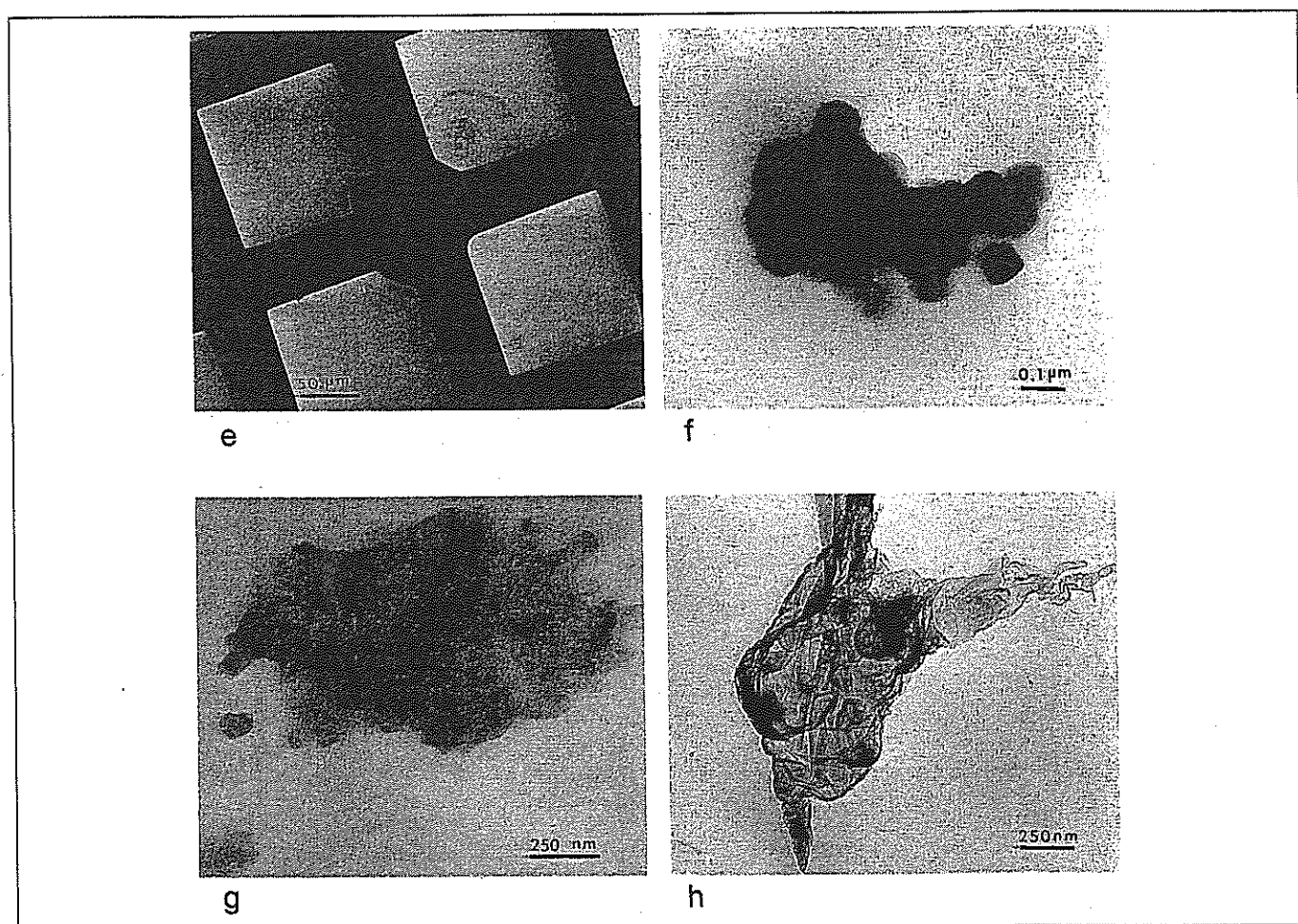


Figure 4. (cont.) (e) Air sample collected during a calm night on a grid (TEM). (f) Crystal aggregate air sample (TEM). Overlapped shadows of crystals are shown on the right upper and lower corners. (g) Agglomerate of different sizes of very tiny crystals (< 10 nm) with organic material is clearly shown (TEM). (h) Folded shape of organic tube with a few inorganic materials (TEM).

that TPs were very effective in sampling dust in workplace air. They used a nichrome (NiCr) wire that was heated electrically to 100°C and the dust deposit on the cover slit was evaluated by light microscopy. According to Maynard,²³ construction of an ultrafine aerosol sampler with unity collection efficiency from $d < 1$ nm up to $d \approx 50$ nm is possible for the particles with $\text{Kn} \gg 1$ (nanoparticles) even though diffusions would be a dominant force for particles with a diameter less than 5 nm. For $\text{Kn} < 1$, Brock²⁴ states that the theoretical upper particle size terminal velocity is independent of the diameter of a particle that extends to over 100 nm.

Apparatus

A TP for direct collection of air particulate matter on grids for TEM study was designed as shown in Figures 1 and 2. It uses characteristics of thermal-gradient (ΔT)-driven adsorption on a transparent formvar-coated substrate (carbon-coated formvar grid) with a 3-mm standard specimen-viewing platform for TEM. The TP utilizes the concept of thermophoresis: particles are bombarded by

higher energy molecules on their "hot" side and thus driven toward the lower temperature zone.

The dimensions of the TP include total weight: 2.41 kg; power usage: 36 W [12 V (car) \times 3.0 amp (2.5 amp for hot wire heater, 0.5 amp for rear fan)]; bottom (supporting) panel ($17.5 \times 13.0 \times 0.6$ cm); cover [6.5×14.0 cm (12.5 cm on top) \times 12.5 cm]; and cold block (copper) ($8.9 \times 8.9 \times 2.5$ cm). A copper block with connected internal cooling coils for water circulation was used for specific cold surface sampling by allowing a standard 3-mm formvar-coated carbon support grid to be placed upon this cold floor. This setup is illustrated in Figure 2a. The fan installed on the rear portion of the cover controlled the overall flow rate of the air such that sampling rates could be adjusted (Figure 2d). A tungsten wire, located directly above the sampling grids above the cold copper block, heats the intake air and generates the ΔT for facilitated sample deposit on the TEM grids (Figure 2b). Values between 1.0×10^5 and 1.2×10^5 K/m for $\Delta T/L$ were employed following the recommendation given in Hinds,²⁵ where ΔT is the temperature

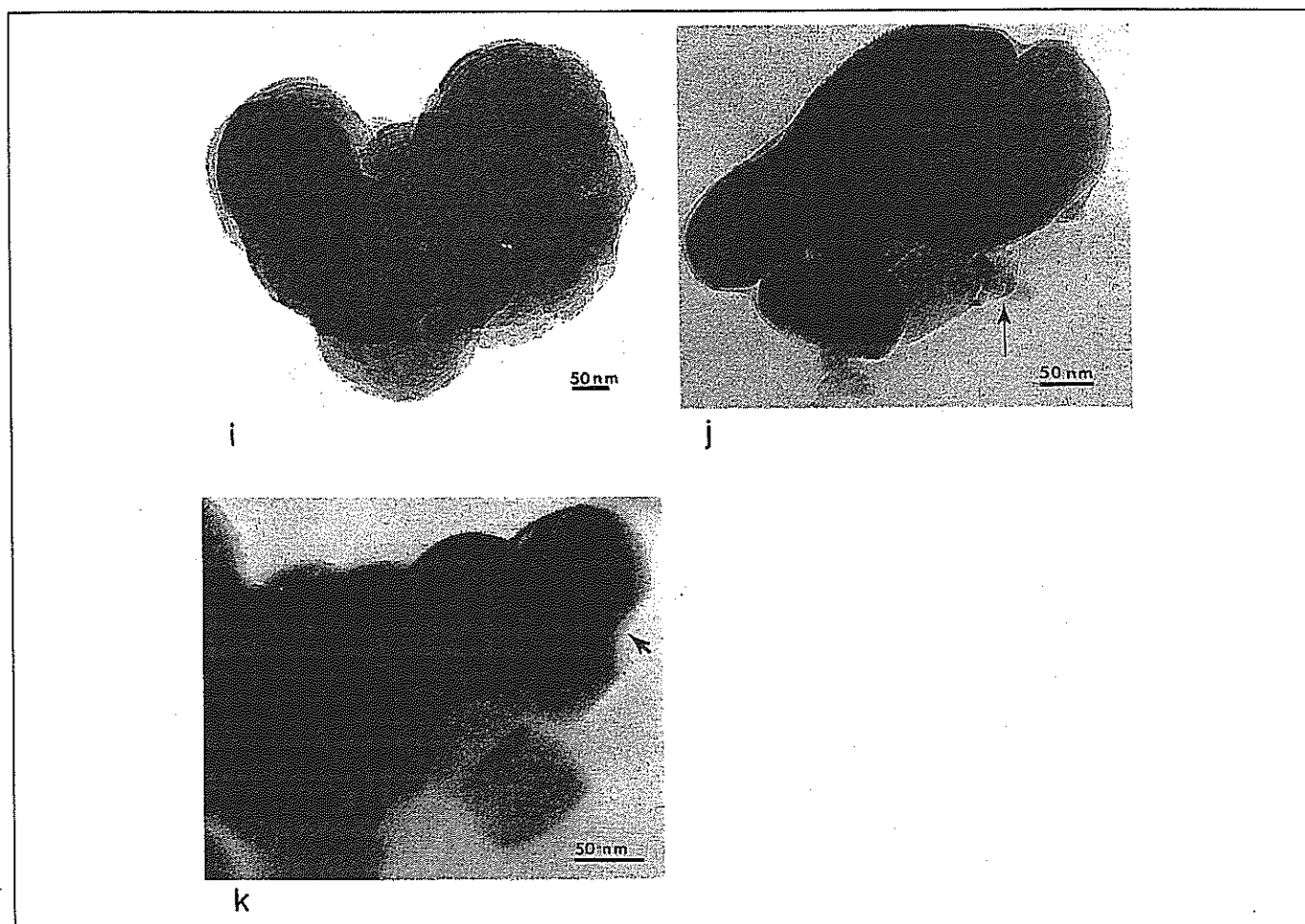


Figure 4. (cont.) (i) Layered agglomerate (TEM). At least two dozen layers of homogeneous materials are shown in this particulate. (j) Arrow shows a very tiny clear crystal in a crystal aggregate (TEM). The size of the crystal shown here is less than 40 nm. (k) Magnified view of (f). On the right top corner, arrow presents overlapped crystals (TEM). Slightly overlapping crystals are also shown on the right lower corner of the picture.

difference (K) between the tungsten hot wire and the cold surface of the copper block where the grid is located, and L is the distance in millimeters between the hot wire and the cold surface where the TEM collection grids are located.

Procedure

After the TP design had been completed, a series of calibration processes using smoke from burning papers and cigarettes, and later TiO_2 rutile powder ($10 \times 50 \text{ nm}$) purchased from a company at Los Alamos, NM, were performed. The airflow rate of the TP was calibrated by using a bubble meter from Gilian Instrument Corp. set between 0 and $1500 \text{ cm}^3/\text{min}$ (0 and $0.05297 \text{ ft}^3/\text{min}$). The temperature of the hot wire and the flow rate of the air were manipulated during the calibration process to find the best combined conditions for sample collection. Particle size-dependent deposition rates as a function of collection grid position (front row vs. rear row, see Figures 1 and 2a) was conducted to find ideal sites for grids using smoke particles from burning papers. TiO_2 powder was

also used to obtain size-specific collection efficiency of the TP used for this study. A series of photographs of various particulates from paper burns, cigarette smoke, and traffic-related and residential air were taken. These are illustrated in Figure 4.

Following the calibration process, field tests were performed to collect numerous representative airborne, sub-micron particulate matter samples ($\text{PM}_{1.0}$). Each test consisted of a 5-min pre-cooling process in which the copper block was cooled by ice-water circulation such that a consistent surface temperature between the block and circulated water was obtained (see Figure 1). Simultaneous to the cooling process, an automobile battery was applied to the tungsten wire for a maximum of 5 min before each sampling process. For each test, at least two grids, one at the center and the others at predetermined lateral positions, were used. After calibration, grids were put only in the front row that showed higher collection efficiency. Each sampling process was performed at approximately 1.5 m above ground level such that actual air inhalation conditions could be approximated. Each sampling period

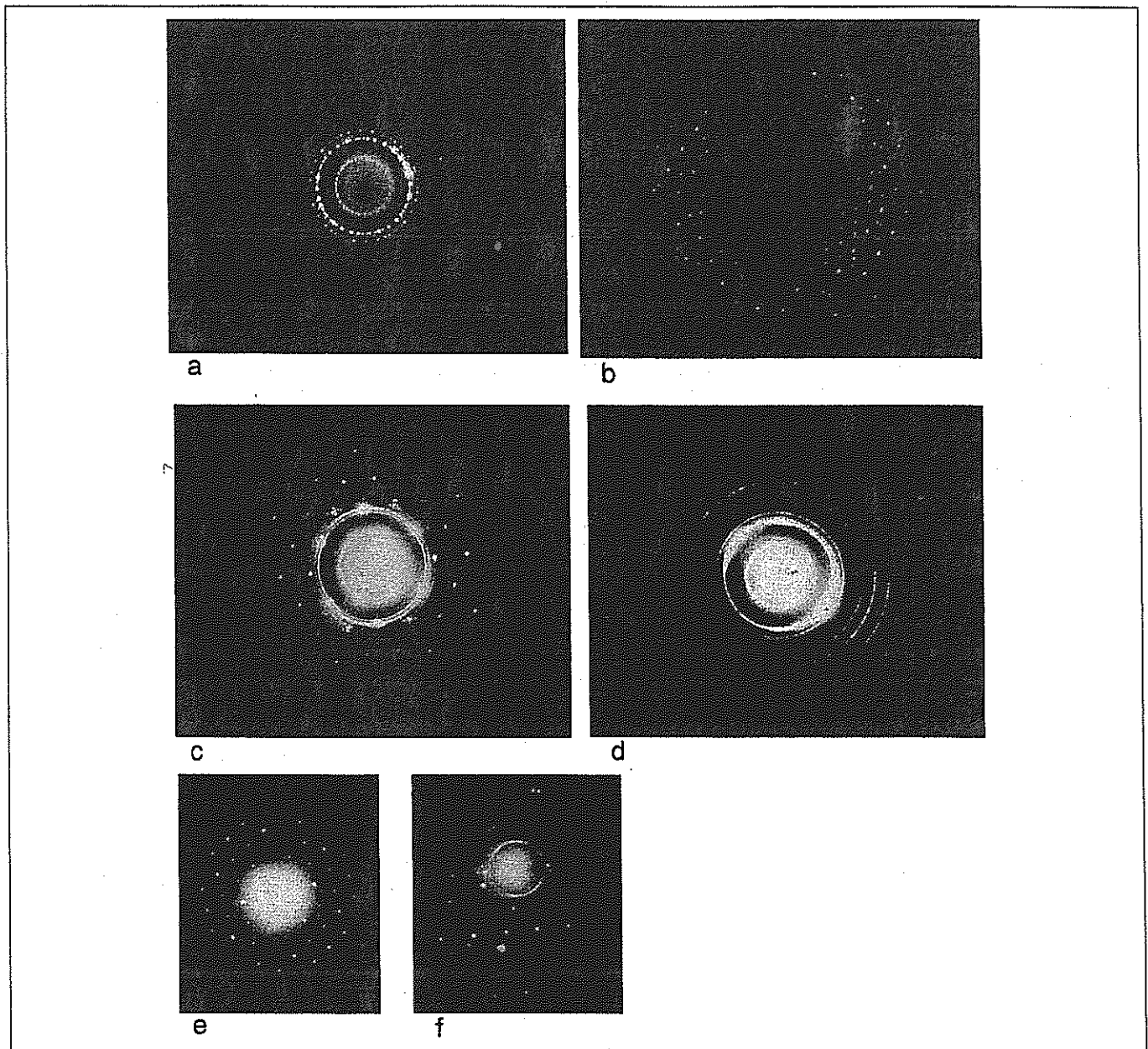


Figure 5. Examples of the variety of SAED patterns for collected particulates. (a) SAED of a combustion air sample from an automobile tailpipe. Crystal texturing. (b) SAED of another combustion air sample from an automobile tailpipe. More than one large single crystal is present. (c) SAED of an aggregate from cigarette smoke. Polycrystals with single crystal. (d) SAED of very small polycrystals. (e) SAED of an evening air sample. Coexistence of single crystal and polycrystal. (f) SAED of a sample collected during sand storm. Polycrystal with single crystal, as in (c).

lasted 30 min. Air samples were collected at different time frames, including consecutive 12-hr overnight sampling in the El Paso, TX, region and various locations in El Paso, including busy traffic intersections, an interstate highway (I-10) along the U.S.–Mexico border, residential areas, and international bridges. During this preliminary study period, more data were collected from central shoulder zones of I-10. The collection was also performed under different weather conditions. Each sample was examined by TEM, and photographs of the samples were taken on every fourth particle encountered during TEM analyses. In addition, EDS studies were performed on each collected

sample for elemental analysis, and some are shown in Figure 6.²⁶ We used a Hitachi-8000 analytical TEM fitted with a goniometer-tilt stage and a NORAN energy-dispersive X-ray spectrometer (EDS) system that is normally operated at 200 KeV with width of the selected area 1.6 μm . For the analyses of aggregate particles, the position of a selected portion in the aggregates was often moved toward the edge of the screen in SAED mode so that other areas in the same aggregate would not be exposed to the beam. This maneuver was performed to maximize the likelihood of examining only the targeted portion of the aggregates of interest.

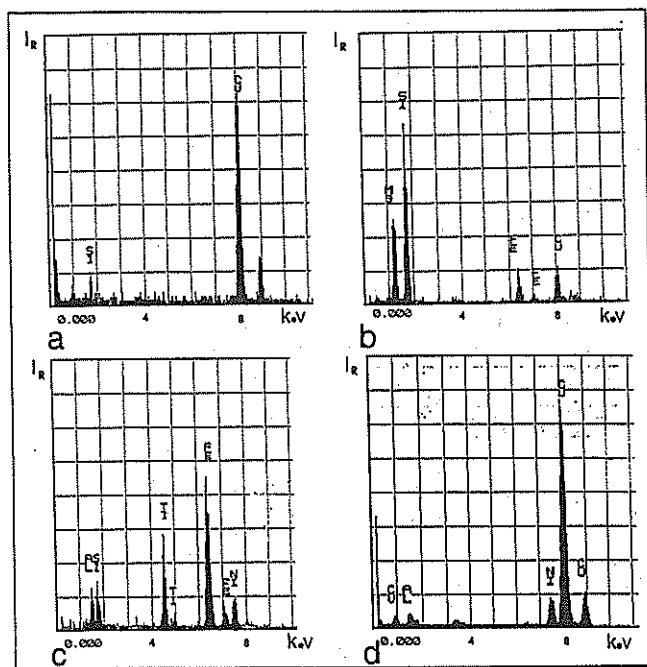


Figure 6. EDS for some representative air samples collected from various locations. (a) Evening residential air sample on a copper grid and the copper peak acts as an internal calibration. The Cu peak is from the grid. (b) An air sample collected at nearby a smelter on a copper grid. (c) An air sample collected nearby a major freeway in El Paso. It shows the examined particulate contained Al, Si, Ti, and Fe. Ni is from Ni grid. (d) An air sample collected at a local traffic intersection on a copper grid.

At the end, a set of R values, that is, the distance between the center spot and the peripheral diffraction spots and rings in the SAED pattern, were measured for the calculation of d spacing values as shown in the formula $L\lambda = Rd$, where $L\lambda$ is a fixed value for a given condition of TEM accelerating voltage (in this study, at 200 KeV), and R is a value that can be physically measured.²⁶ With the data from EDS and the d spacing values, iterative processes between d spacing values of the samples and those of anticipated compounds/molecules were performed to identify the unknowns in the samples examined. Standard d spacings for chemistries were matched with X-ray card file values.

RESULTS AND DISCUSSION

Two different modes of calibration were performed: one using cigarette smoke particles, another using TiO_2 , rutile 10×50 nm. As shown in Figure 3c, the front row collection for particles of the nanometer regime is much more efficient than the rear row of the TP [1804(1225 + 554 + 25) particles vs. 11(0 + 4 + 7)] in terms of particle size-dependent deposition rates as a function of collection grid position. Counting only submicron particles in both rows, close to 98% of the total nano smoke particles collected was located in the front row.

Figures 3d and e show the aggregated and individual form of TiO_2 rutile powder. Figure 3f shows the SAED pattern for the small aggregate in Figure 3d. Only the area surrounded by the black line on the right side was exposed to the testing beam by repositioning the aggregate during SAED mode. Figure 3g is an EDS in the same area that generated the SAED pattern. In the calibration using TiO_2 (nanoparticles), the collection efficiency of the TP reached approximately 86%. The particulates in Figures 4f, g, and j illustrate that many are aggregates of very tiny crystals. These crystals can exhibit catalytic behavior very different from $>1 \mu\text{m}$ particles, especially the large crystals.

The TP used in our investigation was able to collect representative soil components (particulates containing Si, Ca, K, Al, Fe, and Ti) in the air as shown in EDS spectra presented in Figure 6. Anthropogenic elements, including Cu, Zn, and soot, in addition to biological materials, were also collected at various conditions. Individual air PM with different sizes ranging from roughly $10 \mu\text{m}$ to 10 nm for TEM analysis was collected.

During the examination, roughly half of the air particulate samples showed some level of inorganic crystalline characteristics. This is probably because samples had been collected more often in or in close proximity to I-10, where dynamic airflow is always present. Even if it is not exactly clear how these small crystals are associated with some process causing damage to lung tissues and eventual detrimental health issues from respiratory compromise, it is thought that the presence of catalytic reactions facilitated by these small crystals may be required for the generation of agglomerates of PM that show damaging effects. These are the issues that will need to be clarified through further, extensive, interdisciplinary investigations.

The layered air particulate sample presented in Figure 4i drew our attention mainly because of the way that the structure is laid out. This particulate contains dozens of very thin layers (close to 5 nm) of material, most likely graphite. Brake linings are a source of such particulates. The surface area-to-volume ratio of particulates like this structure would be greater than those of other typical air particulates, even complex aggregates. The potential impact of this type of particulate on human lung cells, especially when they have any intrinsic cellular damaging component, also has been raised.²⁷⁻²⁹

Figure 4d shows a polycrystalline SAED pattern for a particle collected with calibrating smoke. The possibly polycrystalline characteristics of smoke-related particles are probably by either contamination or interaction with another airborne inorganic particle during the 10-min period in the confined room where the calibration was performed.

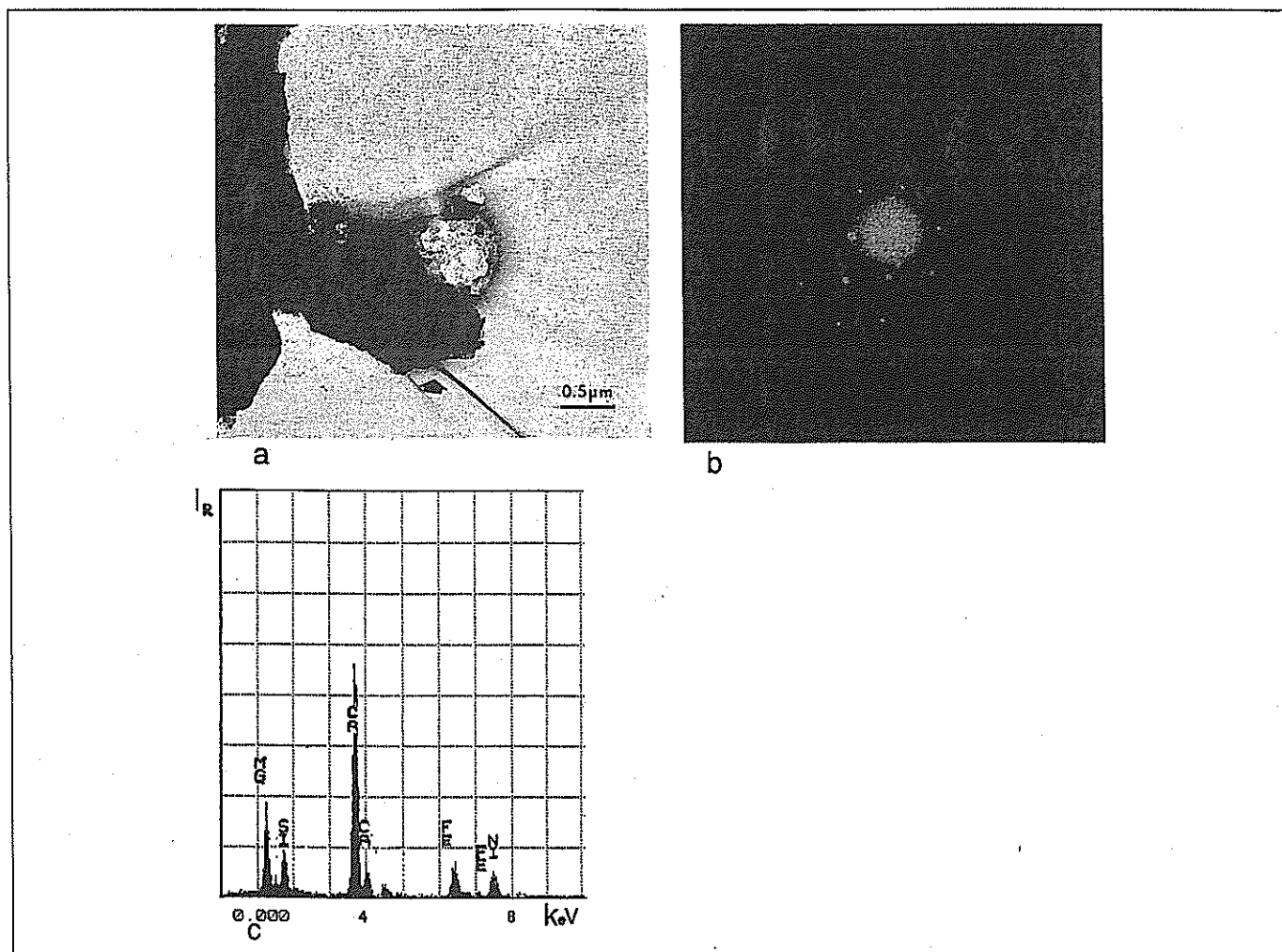


Figure 7. Identified air PM collected in a field test. (a) Air sample identified as $\text{Ca}_2\text{MgFe}_2\text{O}_6$ (TEM). Curved arrows indicate the boundary cut out to include only the small area (pointed by a straight arrow) for the SAED and EDS studies. (b) SAED of $\text{Ca}_2\text{MgFe}_2\text{O}_6$. R values (pattern radii) were used to calculate d spacing values for identification purposes. (c) EDS of the air sample showing peaks for different elements.

The examples of the variety of crystalline particles or variations in crystallinity are illustrated in Figure 5 for comparison with Figure 4. The SAED pattern examples in Figure 5 show large single crystals, tiny polycrystalline aggregates, and mixtures of large crystals and small polycrystals of the same and different compositions, or crystal structures.

In the field tests, the TEM analysis using the samples from the TP with additional data from SAED, EDS, and d spacing values helped in identification of complex particulates. One of them is presented in Figure 7: calcium magnesium iron oxide ($\text{Ca}_2\text{MgFe}_2\text{O}_6$). For $\text{Ca}_2\text{MgFe}_2\text{O}_6$, the eight d spacing values ($d_1 = 3.167 \text{ \AA}$, $d_2 = 2.714 \text{ \AA}$, $d_3 = 2.680 \text{ \AA}$, $d_4 = 2.080 \text{ \AA}$, $d_5 = 1.740 \text{ \AA}$, $d_6 = 1.330 \text{ \AA}$, $d_7 = 1.050 \text{ \AA}$, and $d_8 = 0.870 \text{ \AA}$) calculated from measured R values were matched with those of $\text{Ca}_2\text{MgFe}_2\text{O}_6$ at the card file (Figures 7a, b, and c). Oxygen in this potential structure was not present on EDS. Silicon shown on EDS was not part of the structure identified. The sensitivity of

EDS for elements with atomic number lower than 9 has been inconsistent, and that issue was discussed in Barbi.³⁰

Developing a database that holds characteristics of identifiable individual particles in the ambient air would help recognition of characteristic patterns considered as valuable information to resolve the PM issues we have been dealing with. In that context, this study showed the possibility of characterizing and potentially identifying individual particles using SAED and EDS data from sub-micron particles collected by the TP.

With the benefit of having a way to collect individual air particulates using a grid that can be directly observed under a TEM, this study also showed the possibility of conducting research using selectively chosen individual particulates. In both in vivo and in vitro cases, the validity of data from each study would be much higher and specific when more precisely simulated particles are used. Smith and Aust³¹ and Hughes et al.³² conducted studies that revealed one very valuable piece of information

about the roles of irons and a group of individual metal oxides on cellular toxicity. If data about specific forms of iron of their interest had been available and specifically used, the result of their studies might have been more conclusive.

In conclusion, this preliminary investigation, using the SAED data from the individual particles collected by a thermal precipitator, has demonstrated the potential of characterizing individual air PM in the nanometer scale, and of identifying the components via combined analysis of TEM, SAED, and EDS. More follow-up studies are anticipated to clarify some speculations used in this study and to help resolve specific particulate issues associated with respiratory episodes.

ACKNOWLEDGMENTS

The authors thank Drs. R.R. Chianelli, J. Gardea, and W.W. Li at the University of Texas at El Paso for the many helpful comments they made on this manuscript and David Brown for his technical support in constructing the TP. This project was funded by the Texas Tobacco Industry Settlement, a Mr. and Mrs. MacIntosh Murchison Endowment, a U.S. Environmental Protection Agency (EPA)-Southwest Center for Environmental Research and Policy Project A-02-5, and an EPA-STAR fellowship award (Project U-91609601-0).

REFERENCES

- Levy, J.I.; Hammitt, J.K.; Spengler, J.D. Estimating the Mortality Impacts of Particulate Matter: What Can Be Learned from Between-Study Variability; *Environ. Health Perspect.* **2000**, *108* (2), 109-117.
- Churg, A.; Brauer, M.; Vedal, S.; Stevens, B. Ambient Mineral Particles in the Small Airways of the Normal Human Lung; *J. Environ. Med.* **1999**, *1* (1), 39-45.
- Monarca, S.; Crebelli, R.; Feretti, D.; Zanardini, A.; Fuselli, S.; Filini, L. Mutagens and Carcinogenesis in Size-Classified Air Particulates of a Northern Italian Town; *Sci. Total Environ.* **1997**, *205* (2-3), 137-144.
- Madden, M.C.; Thomas, M.J.; Ghio, A.J. Acetaldehyde Production in Rodent Lung after Exposure to Metal-Rich Particles; *Free Radical Biol. Med.* **1999**, *26* (11-12), 1569-1577.
- Smith, K.R.; Aust, A.E. Mobilization of Iron from Urban Particulates Leads to Generation of Reactive Oxygen Species In Vitro and Induction of Ferritin Synthesis in Human Epithelial Cells; *Chem. Res. Toxicol.* **1997**, *10* (7), 828-834.
- Ding, M.; Shi, X.; Castranova, V.; Vallyathan, V. Predisposing Factors in Occupational Lung Cancer: Inorganic Minerals and Chromium; *J. Environ. Pathol. Toxicol. Oncol.* **2000**, *19* (1-2), 129-138.
- Ding, M.; Shi, X.; Lu, Y.; Huang, C.; Leonard, S.; Roberts, J. Induction of Activator Protein-1 through Reactive Oxygen Species by Crystalline Silica in JB6 Cells; *J. Biol. Chem.* **2001**, *276* (12), 9108-9114.
- Chianelli, R.R.; Yacaman, M.J.; Arenas, J.; Aldape, F. Atmospheric Nanoparticles in Photocatalytic and Thermal Production of Atmospheric Pollutants; *J. Hazard. Sub. Res.* **1998**, *1*, 1-16.
- Renwick, L.C.; Donaldson, K.; Clouter, A. Impairment of Alveolar Macrophage Phagocytosis by Ultrafine Particles; *Toxicol. Appl. Pharmacol.* **2001**, *172* (2), 119-127.
- Green, H.L.; Watson, H.H. *Medical Research Council Special Report*; 199; HMS: London, 1995.
- Einstein, A. *Z. Phys.* **1924**, *27*, 1.
- Prejafon, E.; Kasparian, J.; Fambaldi, P.; Yu, J.; Vezin, B.; Wolf, J.P. Three-Dimensional Analysis of Urban Aerosols by Use of a Combined Lidar, Scanning Electron Microscopy, and X-Ray Microanalysis; *Appl. Optics* **1998**, *37* (12), 2231-2237.
- Ebert, M.; Weinbruch, S.; Hoffmann, P.; Ortner, H.M. Chemical Characterization of North Sea Aerosol Particles; *J. Aero. Sci. Mau.* **2000**, *31* (5), 613-632.
- Rosinski, L.C.; Morgan, G.; Weickmann, P.; Baird, J.; Lecinski, A.; Murr, L.E. A Study of the Population of Ice-Forming Nuclei in New Mexico, U.S.A., and Its Possible Dependence on Meteorological Processes; *Meteorol. Res.* **1981**, *34*, 77-90.
- Petzold, A.; Strom, J.; Ohlsson, S.; Schoroder, F.P. Elemental Composition and Morphology of Ice-Crystal Residual Particles in Cirrus Clouds and Contrails; *Atmos. Res.* **1998**, *49* (1), 21-34.
- Murr, L.E.; Kinard, W.H. Effects of Low Earth Orbit; *Amer. Sci.* **1993**, *81*, 152-165.
- Maynard, A.D.; Brown, L.M. The Collection of Ultrafine Aerosol Particle for Analysis by Transmission Electron Microscopy, Using a New Thermophoretic Precipitator; *J. Aerosol. Sci.* **1991**, *22* (Suppl. 1), S379-S382.
- Katrinak, K.A.; Anderson, J.R.; Buseck, P.R. Individual Particle Types in the Aerosol of Phoenix, Arizona; *Environ. Sci. Technol.* **1995**, *29*, 321-329.
- Understanding the Health Effects of Components of the Particulate Matter Mix: Progress and Next Steps; *HEI Perspect.* **2002**, *April*, 1-20.
- Fubini, B.; Nanetti, G.; Altilla, S.; Tiozzo, R.; Lison, D.; Saffiotti, U. Relationship between Surface Properties and Cellular Responses to Crystalline Silica: Studies with Heat-Treated Cristobalite; *Chem. Res. Toxicol.* **1999**, *12* (8), 737-754.
- Kuhrs, C.; Arita, Y.; Weiss, W.; Ranke, W.; Schlogl, R. Understanding Heterogeneous Catalysis on an Atomic Scale: A Combined Science and Reactivity Investigation for the Dehydrogenation of Ethylbenzene over Iron Oxide Catalysts; *Top. Catal.* **2001**, *14* (1), 111-123.
- Seinfeld, J.H.; Pandis, S.N. *Atmospheric Chemistry and Physics: From Air Pollution to Climate Change*; Wiley & Sons, Inc.: New York, 1996.
- Maynard, A.D. Ph.D. Thesis. Cambridge University, Cambridge, UK, 1992.
- Brock, J.R. On the Theory of Thermal Forces Acting on Aerosol Particles; *J. Colloid Sci.* **1962**, *17*, 768-780.
- Hinds, W.C.; *Aerosol Technology*, 2nd ed.; Wiley & Sons, Inc.: New York, 1999.
- Murr, L.E. *Electron & Ion Microscopy & Microanalysis—Principles and Applications*, 2nd ed.; Marcel Dekker, Inc.: New York, 1991.
- Banfield, J.F.; Welch, S.A.; Xiang, H.; Ebert, T.T.; Penn, L. Aggregation-Based Crystal Growth and Microstructure Development in Natural Iron Oxyhydroxide Biomineralization Products; *Science* **2000**, *289*, 751-754.
- Hart, G.A.; Hesterberg, T.W. In Vitro Toxicity of Respirable-Size Particles of Diatomaceous Earth and Crystalline Silica Compared with Asbestos and Titanium Dioxide; *J. Occup. Environ. Med.* **1998**, *40* (1), 29-41.
- Fubini, B. Surface Reactivity in the Pathogenic Response to Particulates; *Environ. Health Perspect.* **1997**, *105* (5), 1013-1020.
- Barbi, N. *Electron Probe Microanalysis Using Energy Dispersive X-Ray Spectroscopy*; Princeton Gamma-Tech: Princeton, NJ, 1980.
- Smith, K.R.; Aust, A.E. Mobilization of Iron from Urban Particulates Leads to Generation of Reactive Oxygen Species In Vitro and Induction of Ferritin Synthesis in Human Epithelial Cells; *Chem. Res. Toxicol.* **1997**, *10* (7), 828-834.
- Hughes, L.S.; Cass, G.R.; Gone, J.; Ames, M.; Olmez, I. Physical and Chemical Characterization of Atmospheric Ultrafine Particles in the Los Angeles Area; *Environ. Sci. Technol.* **1998**, *32* (9), 1153-1161.

About the Authors

John J. Bang, M.D., is a Ph.D. candidate in the environmental science and engineering program and a research associate under Dr. Murr at the University of Texas at El Paso. Elizabeth A. Trillo, Ph.D., was an adjunct professor in the Metallurgical and Materials Engineering Department at the University of Texas at El Paso and now works as a research engineer consultant at InterCorr International. Lawrence E. Murr, Ph.D. (corresponding author), is a chairman and Mr. and Mrs. MacIntosh Murchison Professor in the Metallurgical and Materials Engineering Department, University of Texas at El Paso, El Paso, TX 79968.